



OPEN Evaluation of thermal effects of surgical energy devices: ex vivo study

Toshiharu Morikawa¹, Shuzo Hamamoto^{1✉}, Masakazu Gonda², Kazumi Taguchi³, Rei Unno¹, Koei Torii¹, Masahiko Isogai¹, Kengo Kawase¹, Takashi Nagai¹, Shoichiro Iwatsuki¹, Toshiki Etani¹, Taku Naiki⁴, Atsushi Okada¹ & Takahiro Yasui¹

This study evaluated the direct and indirect thermal effects of various surgical energy devices using an ex-vivo model. Two types of three devices were evaluated: ENSEAL™ X1 Curved Jaw Tissue Sealer (X1) and ENSEAL™ G2 Curved Tissue Sealer (G2) as vessel sealing systems (VSSs), and HARMONIC® HD1000i Shears (HA) as an ultrasonic activating device (USAD). Each device was activated once under DRY or WET conditions. The tissue's maximum temperature (MT), steam MT surrounding the activation site, and steam spread area (SSA) were measured. Under WET conditions, the median MT of a porcine common carotid artery at 1 mm from the activation site by X1, G2, and HA were 84.4, 83.3, and 50.5 °C, respectively. The direct thermal effect of HA was the lowest among the three devices. VSSs showed higher tissue MT under WET conditions compared with DRY conditions. Conversely, USAD showed the opposite trend. G2 demonstrated a significantly higher MT than X1 and HA ($P < 0.05$). A significant decrease in SSA was observed with decreasing grasping range. In conclusion, VSSs generated higher temperatures than USAD, especially under WET conditions. Surgeons should consider minimizing thermal effects by creating DRY conditions or performing gradual incisions when using VSS devices.

Keywords Vessel sealing system, Ultrasonic activating device, Thermal effect, Grasping range, Steam spread area, WET condition

Abbreviations

X1	ENSEAL™ X1 Curved Jaw Tissue Sealer
G2	ENSEAL™ G2 Curved Tissue Sealer
HA	HARMONIC® HD1000i Shears
VSSs	Vessel sealing systems
USADs	Ultrasonic activating devices
MT	Maximum temperature
DT46	Duration above 46 °C
SSA	Steam spread area

Energy devices are widely utilized across various surgical specialties, facilitating dissection and hemostasis during open and endoscopic procedures^{1–3}. These devices enable surgeons to perform procedures with greater precision and with less bleeding^{4,5}.

Many energy devices exist, including commonly used monopolar instruments, radiofrequency ablation devices, and laser surgical tools. It is well known that bipolar instruments heat up more intensely than monopolar instruments, which in turn heat up more than ultrasonic instruments^{6–10}. Previous studies have extensively evaluated the thermal spread and safety margins of these devices in various surgical situations. Sutton et al. reported that monopolar or bipolar diathermy showed a significantly larger lateral thermal spread than both vessel-sealing systems (VSSs) and ultrasonic activating devices (USADs), indicating higher risks of collateral damage⁶. Similarly, Hefermehl et al. demonstrated that USADs generated the least amount of lateral heat spread

¹Department of Nephro-urology, Nagoya City University Graduate School of Medical Sciences, 1, Kawasumi, Mizuho-cho, Mizuho-ku, Nagoya 467–8601, Japan. ²Department of Urology, Nagoya City University Midori Municipal Hospital, Nagoya, Japan. ³Department of Urology, Nagoya City University East Medical Center, Nagoya, Japan. ⁴Department of Urology, Nagoya City University West Medical Center, Nagoya, Japan. ✉email: hamamoto10@med.nagoya-cu.ac.jp

compared to other devices, supporting their safer profile in terms of thermal injury⁷. Moreover, Türkan et al. highlighted that different energy devices have varying impacts on surgical margins, emphasizing the need to consider these characteristics when selecting a device⁸. Although these studies provide valuable insights, comprehensive comparative data under both DRY and WET conditions remain limited, warranting further investigation. In laparoscopic surgery, VSSs and USADs are particularly prevalent for sealing vessels. Although monopolar energy devices are also commonly used for certain surgical procedures, they are not typically used for vessel sealing because of their inferior sealing capabilities compared with VSSs and USADs^{11,12}. Thus, the current study focused on devices specifically used for vessel sealing to assess their thermal effects on surrounding tissues. VSSs use advanced bipolar devices to fuse the intimal layers of vascular structures through the thermal denaturation of tissue proteins. Notably, this technology undergoes continuous development, allowing for real-time energy delivery optimization based on changing tissue conditions, limiting stray current and reducing heat spread compared with conventional energy devices¹³. Conversely, USADs use high-frequency ultrasound waves to coagulate and incise vessels and tissues¹⁴. This transection effect arises from the mechanical interaction between the oscillating device tip and the tissue, generating less heat than VSSs during activation^{15–17}.

Despite their widespread adoption, energy devices for hemostasis possess potential disadvantages, including surrounding thermal effects¹⁸. Temperatures exceeding 46 °C are reported to cause cellular injury¹⁹, while exposure above 60 °C can lead to nerve injury²⁰. Furthermore, thermal effects generated by these devices can be analyzed from two perspectives: direct thermal conduction and indirect steam thermal effect. Notably, within the urological field, the use of VSSs during robotic-assisted radical prostatectomy remains controversial because it may cause nerve injuries that could lead to retractile dysfunction and urinary incontinence^{21,22}. However, data on lateral thermal spread associated with energy devices are limited. Therefore, this study aimed to evaluate the direct and indirect thermal spread of various energy devices under various conditions using an ex-vivo model (Fig. 1).

Results

Evaluation of the direct thermal effect

Figure 2A displays the continuous temperature changes following X1 activation. Both the MT and duration above 46 °C (DT46) were calculated. As shown, the temperature rapidly increases during activation before gradually decreasing. The MT during X1 activation is shown in Fig. 3A. Under DRY conditions, the median MT [range] at 1, 3, and 5 mm away from the activation site were 58.7 [49.2–68.9], 46.6 [39.3–55.9], and 36.4 [31.3–39.5] °C, respectively. Under WET conditions, the median MT [range] at 1, 3, and 5 mm away from the activation site were 84.4 [77.7–87.8], 74.1 [62.3–84.1], and 47.1 [39.2–55.9] °C, respectively. These values significantly decreased with increasing distance ($P < 0.05$). Notably, the MT was significantly higher in WET than in DRY conditions at all distances. Importantly, temperatures exceeding 46 °C were not observed at the 5 mm point under DRY conditions, and temperatures exceeding 60 °C were not observed at any point under either condition.

Figure 3B compares the MT at 1 mm from the activation site for all devices under both DRY and WET conditions. Under DRY conditions, the median MT [range] during the activation of X1, G2, and HA were 58.7 [49.2–68.9], 68.0 [61.0–75.6], and 56.6 [48.0–70.7], respectively. The MT in group G2 was significantly higher than that in groups X1 and HA. Moreover, no significant differences were observed between the X1 and HA groups. Under WET conditions, the median MT were 84.4 [77.7–87.8], 83.3 [75.0–91.1], and 50.5 [45.2–55.9] °C for X1, G2, and HA, respectively. Notably, the MT of HA was significantly lower than G2 ($P < 0.05$). X1 and G2 exhibited significantly higher MT under WET conditions compared to DRY conditions, while HA displayed the opposite trend, with significantly lower MT under DRY conditions. Importantly, temperatures exceeding 60 °C were rarely observed in the HA group under DRY conditions and were absent under WET conditions.

Table 1 presents the median DT46 values for the direct thermal effect. Under DRY conditions, the median DT46 at 1 mm point from the activation site of X1, G2, and HA were 17.5 [0.0–23.0], 19.5 [15.0–26.0], and 9.0 [3.0–17.0] seconds, respectively. HA had the shortest DT46 among the three groups ($P < 0.05$). Under WET conditions, the median DT46 were 18.0 [17.0–31.0], 19.0 [16.0–27.0], and 5.0 [0.0–7.0] seconds for X1, G2, and HA, respectively, with HA again demonstrating the shortest DT46 ($P < 0.05$). The DT46 of HA under DRY conditions was significantly longer than that under WET conditions.

Evaluation of the indirect steam thermal effect

Continuous temperature changes at 1, 5, and 10 mm away from the X1 activation site were monitored, as shown in Fig. 2B. Compared with the direct thermal effect, the temperatures tended to rise and drop more quickly. Figure 4A displays the MT after X1 activation under DRY and WET conditions. Under DRY conditions, the median MT [range] at 1, 5, and 10 mm away from the activation site were 55.4 [45.0–77.0], 37.8 [33.3–46.5], and 32.2 [27.4–41.0] °C, respectively. Under WET conditions, the median MT [range] at 1, 5, and 10 mm away from the activation site were 74.1 [53.5–84.7], 38.1 [24.8–60.0], and 26.0 [24.4–46.4] °C, respectively. Further, MT significantly increased with increasing distance from the grasping site (1, 5, and 10 mm); however, no significant differences were observed between MT at different distances inside/outside the activation zone or between DRY and WET conditions. Temperatures exceeding 46 °C were rarely observed beyond 5 mm, and no temperatures > 60 °C were detected.

Figure 4B illustrates MT for all devices at 1 mm from the activation site under DRY and WET conditions. Under DRY conditions, the median MT for X1, G2, and HA were 55.7 [53.9–76.2], 71.3 [68.7–79.6], and 59.5 [57.5–61.1] °C, respectively. The MT in group G2 was significantly higher than that in group HA ($P < 0.05$). Under WET conditions, the median MT were 74.5 [67.4–83.7], 69.5 [66.4–88.6], and 48.7 [42.0–60.4] °C, respectively. Again, HA displayed significantly lower MT than in groups X1 and G2 ($P < 0.05$).



Fig. 1. (A) Energy devices employed in this study: ENSEAL™ G2 Curved Tissue Sealer, HARMONIC® HD1000i Shears, and ENSEAL™ X1 Curved Jaw Tissue Sealer (from top to bottom). (B) Six-channel model of AM-9000 K thermocouple. (C) An ex-vivo model analyzing the direct thermal effect. A pin electrode was placed into the tissue, and the temperature was recorded at 1, 3, and 5 mm away from the energy device. (D) An ex-vivo model analyzing the indirect steam thermal effect. A pin electrode was placed above the jaw grasping tissue, and the temperature of the surrounding space was recorded at six different points from the grasping site (1, 5, and 10 mm of the outside (a) and inside (b)). (E) An ex-vivo model analyzing the steam thermal spread of energy devices. Versatile Training Tissue (VTT), whose color changes from brown to white at approximately 50 °C, was located horizontally (a) and vertically (b). The center of the VTT was grasped and activated once an energy device was used. (F) VTT after activation of energy device (a: horizontal sheet, b: vertical sheet). The steam spread area was calculated by the sum of the white areas of both horizontal and vertical sheets.

The median DT46 values against the indirect steam effect are shown in Table 2. Under DRY conditions, the median DT 1 mm HA had the shortest DT46 at 1 mm ($P < 0.05$) compared to the other devices, while X1 exhibited shorter DT46 than G2. No significant differences were observed among the groups at distances > 5 mm. Under the WET conditions, HA again demonstrated the shortest DT46 at 1 mm, but no significant difference existed between X1 and G2.

Evaluation of the steam spread by energy device

Figure 5A presents the median SSA generated by X1 at 10 mm, 15 mm, and full bite grasping ranges. SSA also significantly increased, with median values [range] of 120.6 [15.8–132.6], 171.0 [128.4–248.1], and 306.9 [264.6–336.5] mm², respectively. Figure 5B shows the SSA for each device with a 15 mm grasping range. Notably, G2 exhibited significantly higher SSA than HA ($P < 0.05$), while its SSA trended higher than X1's, although not statistically significant.

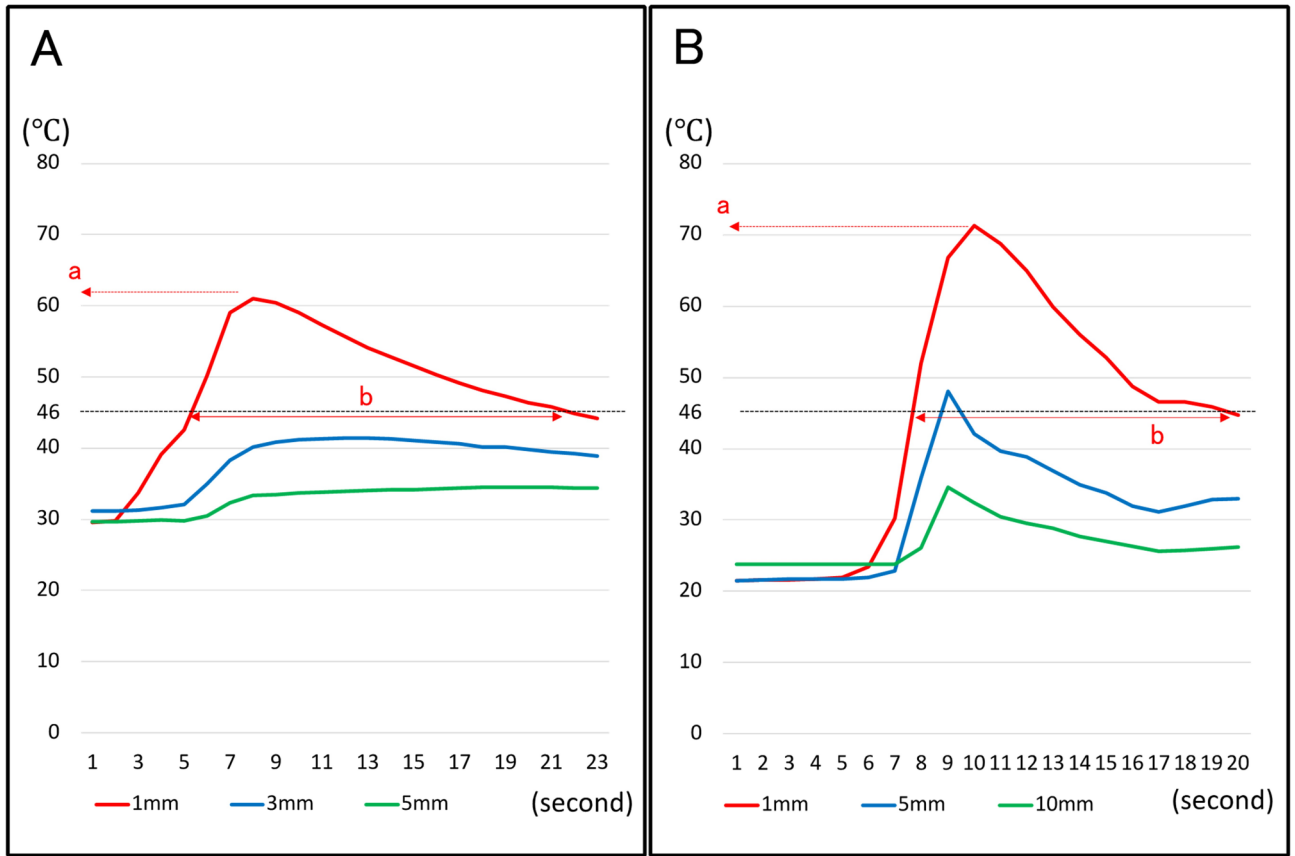


Fig. 2. Continuous temperature changes after activation of energy device against direct thermal effect (A) and indirect steam thermal effect (B): (a) indicates the maximum temperature at 1 mm away from the activation site; (b) indicates the duration time exceeding 46 °C at 1 mm away from the activation site.

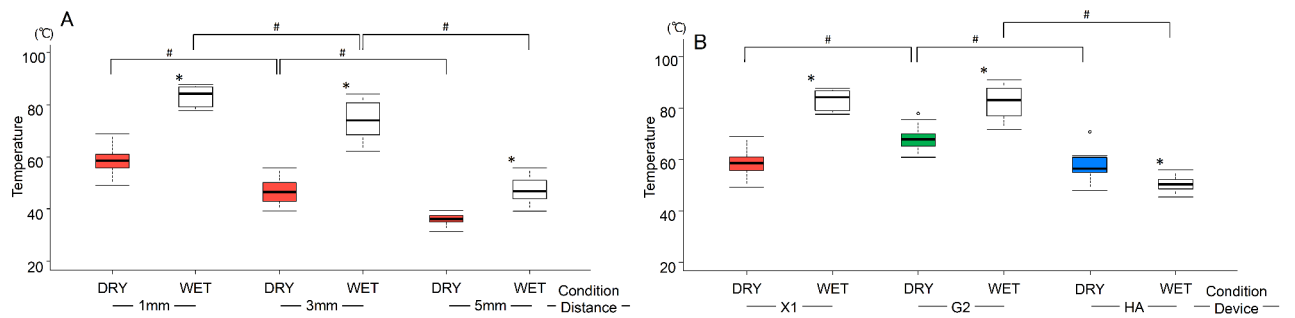


Fig. 3. Results of an ex-vivo study of direct thermal effect. (A) Maximum temperature (MT) during ENSEAL™ X1 (X1) activation at 1, 3, and 5 mm away from the device under DRY and WET conditions. Under DRY conditions, MT decreased significantly with increasing distance under both DRY and WET conditions. MT under WET conditions was significantly higher than that under DRY conditions. (B) MT at 1 mm point from the activation site by all devices (X1, ENSEAL™ G2 (G2), HARMONIC HD1000i (HA)) under DRY and WET conditions. MT in group G2 was significantly higher than in groups X1 and HA under DRY conditions. MT in group HA was significantly lower than in groups X1 and G2 under WET conditions. MT in groups X1 and G2 under WET conditions were significantly higher than those under DRY conditions. On the other hand, MT in groups HA under DRY conditions was significantly lower than that under WET conditions. * indicates a significant difference between DRY and WET conditions at a P-value of 0.05. # indicates a significant difference at a P-value of 0.05.

DRY/WET condition	Distance from activation site (mm)	X1 (sec)	G2 (sec)	HA (sec)	P-value
DRY	1	17.5 (0.0–23.0)	19.5 (15.0–26.0)	9.0 (3.0–17.0)	< 0.05
WET	1	18.0 (17.0–31.0)	19.0 (16.0–27.0)	5.0 (0.0–7.0)	< 0.05
DRY	3	3.5 (0.0–18.0)	17.5 (0.0–26.0)	0.0 (0.0–13.0)	< 0.05
WET	3	17.5 (16.0–30.0)	18.0 (15.0–25.0)	0.0 (0.0–6.0)	< 0.05
DRY	5	0.0 (0.0–0.0)	0.0 (0.0–19)	0.0 (0.0–0.0)	0.12
WET	5	7.0 (0.0–18.0)	0.0 (0.0–18.0)	0.0 (0.0–0.0)	< 0.05

Table 1. Median duration time over 46 °C against the direct thermal effect of energy devices. X1: ENSEAL X1; G2: ENSEAL G2; HA: HARMONIC; sec: seconds; mm: millimeters.

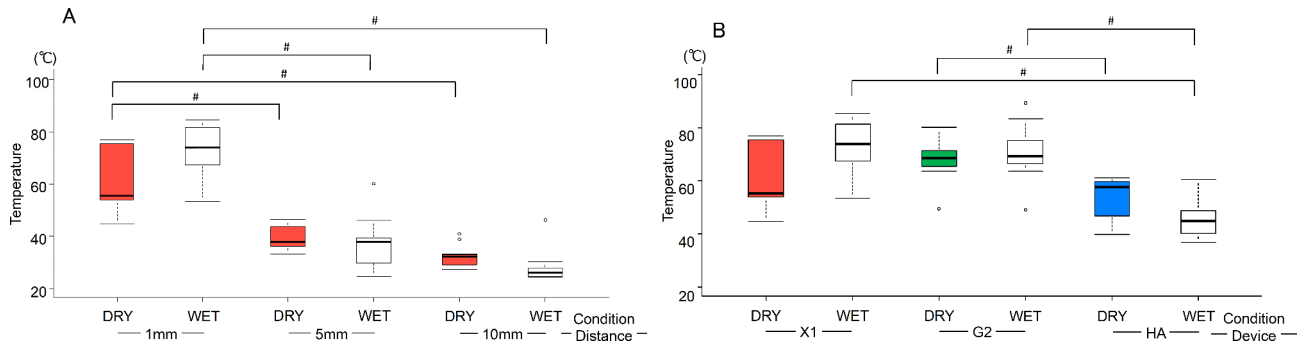


Fig. 4. Results of an ex-vivo study of indirect steam thermal effect. (A) Maximum temperature (MT) during ENSEAL™ X1 (X1) activation at 1, 5, and 10 mm away from the device under DRY and WET conditions. MT significantly increased with increasing distance from the grasping site (1, 5, and 10 mm, respectively). However, no differences were observed in the MT between the two conditions. (B) MT against indirect steam thermal effect of all devices (X1, ENSEAL™ G2 [G2], HARMONIC® HD1000i [HA]) at 1 mm point from the activation site under DRY and WET conditions. MT in group HA was significantly lower than in groups X1 and G2. # Indicates a significant difference at a P-value of 0.05.

DRY/WET condition	Distance from activation site (mm)	X1 (sec)	G2 (sec)	HA (sec)	P-value
DRY	1	9.0 (0.0–15.0)	11.5 (4.0–19.0)	7.5 (0.0–13.0)	< 0.05
WET	1	11.0 (4.0–12.0)	14.5 (4.0–24.0)	0.0 (0.0–7.0)	< 0.05
DRY	5	0.0 (0.0–1.0)	0.0 (0.0–1.0)	0.0 (0.0–0.0)	0.612
WET	5	0.0 (0.0–2.0)	0.0 (0.0–16.0)	0.0 (0.0–0.0)	0.196
DRY	10	0.0 (0.0–0.0)	0.0 (0.0–0.0)	0.0 (0.0–0.0)	N/A
WET	10	0.0 (0.0–1.0)	0.0 (0.0–1.0)	0.0 (0.0–0.0)	0.612

Table 2. Median duration time over 46 °C against the indirect steam thermal effect of energy devices. X1: ENSEAL X1; G2: ENSEAL G2; HA: HARMONIC; sec: seconds; mm: millimeters.

Discussion

In this ex-vivo study, the direct and indirect thermal effects of three types of energy devices (USAD vs. two VSSs) on the surrounding tissues were analyzed. We observed that temperature increased closer to the activation point while the steam-spread area increased with wider grasping ranges. Further, VSSs generally caused higher tissue temperature than USAD, both directly and indirectly. Notably, the temperature during VSS activation was higher under WET conditions than under DRY conditions, whereas USAD had a higher thermal effect under DRY conditions than under WET conditions.

The distinct hemostasis mechanisms of USAD and VSSs contribute to their differing thermal effects on the surrounding tissues. USAD simultaneously coagulates and transects surrounding tissues using a high-frequency vibration system. USAD affects biological tissues through mechanical cutting, drying, and protein coagulation. Ultrasonic cutting results from the mechanical interaction between the vibrating site and the tissue. It uses the mechanism of cavitation. Cavitation is a process in which ultrasound waves are applied to a liquid to generate a vacuum bubble, which generates a shock wave when it collapses. USAD achieves a fusion or cutting effect by vaporizing and rupturing cells in a small and limited area at the tip of the blade via cavitation caused by vibration of the blade, with controlled amplitude and frequency of the moving part. In the present study, HA exhibited fewer direct and indirect thermal effects. However, lower burst pressure reported for USAD suggests

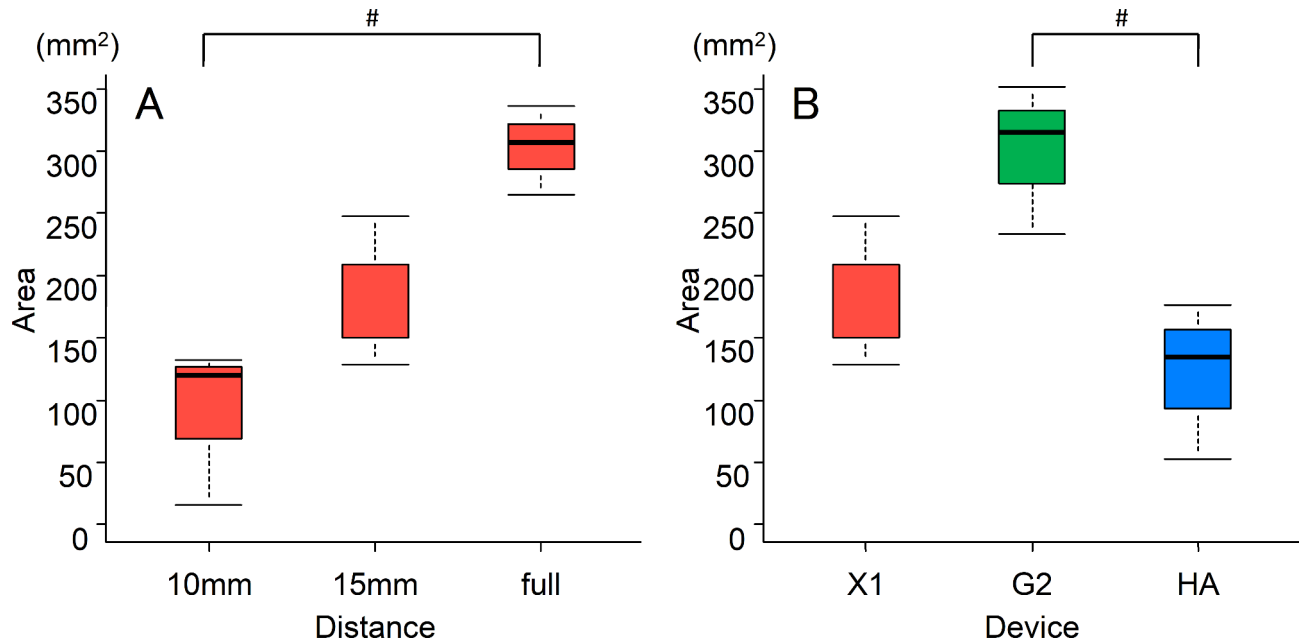


Fig. 5. Results of steam spread area (SSA). (A) Comparison of SSA by grasping ranges 10 mm, 15 mm, and full bite generated by ENSEAL™ X1 (X1). SSA increased significantly with increasing grasping range. (B) The SSA while each device (X1, ENSEAL™ G2 [G2], HARMONIC® HD1000i [HA]) was activating with a 15 mm grasping range. The SSA of G2 was significantly larger than that of HA. The SSA of G2 seemed larger than that of X1. However, no significant difference was observed. # indicates a significant difference at a P-value of 0.05.

weaker sealing than in VSS²³. Tissue sealing and hemostasis with VSS are achieved through tissue compression and alternating polar electric currents that are converted to thermal energy in the tissues. This triggers collagen and elastin denaturation in vessel walls, forming a hemostatic seal²⁴. The presence of water and ions in the tissue causes ion oscillation due to VSS activation, which ultimately converts infrared energy into intracellular heat, resulting in the vaporization of intracellular water and an increase in the temperature of the surrounding tissues¹⁵. However, heat generation can be controlled by adjusting the electrical delivery algorithm. X1 and G2 use different output algorithms. The energy delivery algorithm for X1 had an initial low-heat output that increased gradually along the energy delivery stages, whereas G2 exhibited intermittent high-energy delivery from the start of activation. In this study, the direct thermal effect under DRY conditions was predominantly higher for G2 than for X1, and the spread of steam heat was greater for G2 than for X1. We observed that the difference in the delivery algorithms caused a difference in the generation of steam heat.

This study investigated the thermal effects of energy devices under DRY and WET conditions. Key findings include the following: VSSs generally showed higher temperatures under WET conditions than under DRY conditions, whereas the USADs showed the opposite results. These results align with previous reports¹⁵ and likely reflect differences in device mechanisms between VSSs and USADs. In the case of VSSs, water had a higher temperature under DRY conditions than under WET conditions due to lateral heat propagation caused by current leakage. Conversely, in the case of USADs, it was higher under DRY conditions than under WET conditions due to the cooling of moving parts by the liquid.

All devices showed increased steam-spread area with a larger grasping range (10 and 15 mm, full bite). This may be due to the influence of the increased grasping area, which is affected by the severe thermal effect. However, a previous study reported that temperature increased with a decreased grasping range¹⁷. Hayami et al. concluded that water in the non-grasping zone caused vaporization due to Joule heating and increased temperature in the surrounding tissues. However, a short grasping range is associated with a short activation time; hence, the thermal effect induced by energy devices with various grasping ranges may be limited.

Cellular injury temperatures (46 °C)¹⁹ and nerve injury thresholds (60 °C)²⁰ were rarely exceeded in this study, suggesting potentially safe use within 5 mm of the activation site for all devices. This may be attributed to built-in temperature monitoring mechanisms. Hayami et al. also reported safe distances of 10 mm and 3 mm for VSSs and USADs, respectively¹⁵. These results support the safety of currently used energy devices^{25,26}.

Our study had some limitations. First, our study used an ex vivo model; thus, the thermal effect may differ in tissues with blood flow. Furthermore, the indirect steam spread effect might differ due to gas composition and perfusion in the aeroperitoneum compared with air²⁷. This study only evaluated tissue temperature, which may not fully capture the actual severity of thermal injury, influenced by factors like repeated activation and blade shape^{28,29}. Second, although the HARMONIC® HD1000i Shear was used as a representative USAD in this study, it has recently been replaced by the HARMONIC™ 1100 Shear. However, as the primary difference between the two shears is the maximum blade temperature after the transection is complete³⁰, there might be no effect on the

maximum tissue temperature. Third, in this ex vivo model, there might have been instrumental measurement errors, such as potential measurement delays and the unmeasured heat capacity of the pin electrode.

However, very few studies have investigated the temperature of energy devices under different conditions and devices. While limited by its ex-vivo setting, this study provides a valuable preclinical evaluation for further clinical investigations.

Conclusion

This study revealed that VSSs generate higher thermal effects than USADs. VSS performance was influenced by moisture content, while USADs were affected by frictional heat reduction in wet environments. All devices had some thermal effects, but short grasping ranges and distances exceeding 5 mm from the activation point could potentially minimize this effect. Surgeons may consider using DRY conditions or gradual incision creation to reduce thermal impact further.

Methods

Three energy devices, including two VSSs and a USAD, were compared regarding their direct and indirect thermal effects (Fig. 1A). The two VSSs included an ENSEAL™ X1 Curved Jaw Tissue Sealer (X1; Ethicon, Johnson & Johnson, K.K., New Brunswick, US) and ENSEAL™ G2 Curved Tissue Sealer (G2; Ethicon, Johnson & Johnson). HARMONIC® HD1000i Shears (HA; Johnson & Johnson) was used as the USAD. An ETHICON GEN11 Generator (Ethicon, Johnson & Johnson) was used as the generator system. X1 and G2 were activated in the Default mode, and the Extended Activation mode was not used. HA was activated with a default minimum power level of 3 and maximum power level of 5, and the Advanced Hemostasis mode was not used. An AM-9000 K thermocouple (Anritsu Meter, Tokyo, Japan) was used to measure tissue and steam temperatures. This instrument has a six-channel port, which enables the simultaneous measurement of a maximum of six locations (Fig. 1B). Temperatures were measured using a pin electrode, which was measurable from -40 to $+333$ °C. The laboratory room temperature was maintained at 23 °C.

Evaluation of the direct thermal effect

A porcine common carotid artery was used for this ex-vivo study. The diameter of the artery was approximately 3–5 mm. Each artery was grasped using energy devices and activated once using the energy devices until completion under two conditions: DRY and WET. The devices were activated immediately after removing any surface water in the DRY condition. Conversely, under the WET condition, the devices were activated after immersion in water. Tissue temperature was measured at distances of 1, 3, and 5 mm from the energy device activation point (Fig. 1C). Each condition was repeated 10 times. The maximum temperature (MT) and duration above 46 °C (DT46) were compared across different distances and device types (Fig. 2A).

Evaluation of the indirect steam thermal effect

The temperature of the steam surrounding the activated device was measured using an AM-9000 K thermocouple. Five measurements were taken at distances of 1, 5, and 10 mm outside (Fig. 1D-a) and inside (Fig. 1D-b) the activation zone on pig common carotid arteries. Similar to the direct effect evaluation, the maximum temperature and duration above 46 °C compared across different distances and device types (Fig. 2B). Statistical analyses were performed using a combination of external and internal data.

Evaluation of the steam spread generated from energy devices

The thermal spread of steam generated from energy devices was analyzed using Versatile Training Tissue (VTT), which changes color from brown to white around 50 °C. The VTT was located, as shown in Fig. 1E, with the energy device activated once at its center. The horizontal and vertical discolored areas on the VTT, defining the steam spread area (SSA) (Fig. 1F), were measured using ImageJ software, which is consistent with prior research³¹. The total SSA was calculated by summing these values. Grasping ranges of 10 mm, 15 mm, and full bite were applied under DRY and WET conditions. Each set of conditions was replicated three times.

Statistical analyses

Two physicians (TM and SH) performed all statistical analyses using EZR software, a graphical user interface for R³². Quantitative variables were expressed as median [range], and Mann–Whitney U tests and one-way analysis of variance were used to compare quantitative data. All P-values were two-sided with a significance level of 0.05. Analysis of variance was performed to compare the three groups.

Data availability

The data that support the findings of this study are available from the corresponding author upon reasonable request.

Received: 7 July 2024; Accepted: 4 November 2024

Published online: 09 November 2024

References

1. Massarweh, N. N., Cosgriff, N. & Slakey, D. P. Electrosurgery: history, principles, and current and future uses. *J. Am. Coll. Surg.* **202**, 520–530 (2006).
2. Entezari, K., Hoffmann, P., Goris, M., Peltier, A. & Van Velthoven, R. A review of currently available vessel sealing systems. *Minim. Invasive Ther. Allied Technol.* **16**, 52–57 (2007).

3. Brill, A. I. Bipolar electrosurgery: convention and innovation. *Clin. Obstet. Gynecol.* **51**, 153–158 (2008).
4. Overhaus, M. et al. Efficiency and safety of bipolar vessel and tissue sealing in visceral surgery. *Minim. Invasive Ther. Allied Technol.* **21**, 396–401 (2012).
5. Hamamoto, S. et al. LigaSure versus the standard technique (Hem-o-lok clips) for robot-assisted radical prostatectomy: A propensity score-matched study. *J. Robot Surg.* **15**, 869–875 (2021).
6. Sutton, P. A., Awad, S., Perkins, A. C. & Lobo, D. N. Comparison of lateral thermal spread using monopolar and bipolar diathermy, the harmonic scalpel and the LigaSure. *Br. J. Surg.* **97**, 428–433 (2010).
7. Hefermehl, L. J. et al. Lateral temperature spread of monopolar, bipolar and ultrasonic instruments for robot-assisted laparoscopic surgery. *BJU Int.* **114**, 245–252 (2014).
8. Türkan, A. et al. Effect of LigaSure™, monopolar cautery, and bipolar cautery on surgical margins in breast-conserving surgery. *Breast Care (Basel).* **14**, 194–199 (2019).
9. Diamantis, T. et al. Comparison of monopolar electrocoagulation, bipolar electrocoagulation, Ultracision, and LigaSure. *Surg. Today.* **36**, 908–913 (2006).
10. Khan, F., Rodriguez, E., Finley, D. S., Skarecky, D. W. & Ahlering, T. E. Spread of thermal energy and heat sinks: implications for nerve-sparing robotic prostatectomy. *J. Endourol.* **21**, 1195–1198 (2007).
11. Janssen, P. F., Brölmann, H. A. & Huirne, J. A. Effectiveness of electrothermal bipolar vessel-sealing devices versus other electrothermal and ultrasonic devices for abdominal surgical hemostasis: a systematic review. *Surg. Endosc.* **26**, 2892–2901 (2012).
12. Hubner, M. et al. Prospective randomized study of monopolar scissors, bipolar vessel sealer and ultrasonic shears in laparoscopic colorectal surgery. *Br. J. Surg.* **95**, 1098–1104 (2008).
13. Chekan, E. G., Davison, M. A., Singleton, D. W., Mennone, J. Z. & Hinoul, P. Consistency and sealing of advanced bipolar tissue sealers. *Med. Devices (Auckl).* **8**, 193–199 (2015).
14. Timm, R. W. et al. Sealing vessels up to 7 mm in diameter solely with ultrasonic technology. *Med. Devices (Auckl).* **7**, 263–271 (2014).
15. Hayami, M. et al. Steam induced by the activation of energy devices under a wet condition may cause thermal injury. *Surg. Endosc.* **34**, 2295–2302 (2020).
16. Lambertson, G. R. et al. Prospective comparison of four laparoscopic vessel ligation devices. *J. Endourol.* **22**, 2307–2312 (2008).
17. Hayami, M. et al. Lateral thermal spread induced by energy devices: a porcine model to evaluate the influence on the recurrent laryngeal nerve. *Surg. Endosc.* **33**, 4153–4163 (2019).
18. Nechay, T. et al. Thermal processes in bile ducts during laparoscopic cholecystectomy with monopolar instruments. Experimental study using real-time intraluminal and surface thermography. *Surg. Innov.* **28**, 525–535 (2021).
19. Leber, B. et al. Impact of temperature on cell death in a cell-culture model of hepatocellular carcinoma. *Anticancer Res.* **32**, 915–921 (2012).
20. Lin, Y. C. et al. Electrophysiologic monitoring correlates of recurrent laryngeal nerve heat thermal injury in a porcine model. *Laryngoscope.* **125**, E283–E290 (2015).
21. Penson, D. F. et al. 5-year urinary and sexual outcomes after radical prostatectomy: results from the prostate cancer outcomes study. *J. Urol.* **173**, 1701–1705 (2005).
22. Boorjian, S. A. et al. A critical analysis of the long-term impact of radical prostatectomy on cancer control and function outcomes. *Eur. Urol.* **61**, 664–675 (2012).
23. Goldstein, S. L. et al. Comparison of thermal spread after ureteral ligation with the Laparo-Sonic ultrasonic shears and the LigaSure system. *J. Laparoendosc Adv. Surg. Tech. A.* **12**, 61–63 (2002).
24. Reyes, D. A., Brown, S. I., Cochrane, L., Motta, L. S. & Cuschieri, A. Thermal fusion: Effects and interactions of temperature, compression, and duration variables. *Surg. Endosc.* **26**, 3626–3633 (2012).
25. Kuroda, K. et al. Comparison of short-term surgical outcomes of two types of robotic gastrectomy for gastric cancer: ultrasonic shears method versus the Maryland bipolar forceps method. *J. Gastrointest. Surg.* **27**, 222–232 (2023).
26. Lee, S. H. et al. Comparing the utility and surgical outcomes of harmonic focus ultrasonic scalpel with LigaSure small jaw bipolar device in thyroidectomies: a prospective randomized controlled trial. *Ann. Surg. Oncol.* **26**, 4414–4422 (2019).
27. Siracusano, S. et al. Measuring thermal spread during bipolar cauterizing using an experimental pneumoperitoneum and thermal sensors. *Front. Surg.* **10**, 1115570 (2023).
28. Shibao, K. et al. Repeated partial tissue bite with inadequate cooling time for an energy device may cause thermal injury. *Surg. Endosc.* **35**, 3189–3198 (2021).
29. Kajiwara, S., Noshiro, H., Kitagawa, H., Tanaka, T. & Kai, K. Modification of the thermal spread by the blade shape of an ultrasonically activated device. *World J. Surg.* **45**, 1698–1705 (2021).
30. Kajiwara, M., Fujikawa, T. & Hasegawa, S. Tissue pad degradation of ultrasonic device may enhance thermal injury and impair its sealing performance in liver surgery. *World J. Hepatol.* **14**, 1357–1364 (2022).
31. Schneider, C. A., Rasband, W. S. & Eliceiri, K. W. NIH image to ImageJ: 25 years of image analysis. *Nat. Methods.* **9**, 671–675 (2012).
32. Kanda, Y. Investigation of the freely available easy-to-use software 'EZ' for medical statistics. *Bone Marrow Transpl.* **48**, 452–458 (2013).

Acknowledgements

We are grateful to Editage for carefully proofreading the manuscript.

Author contributions

T Morikawa: writing – original draft (lead); data curation (lead); Methodology (equal); formal analysis (lead). S Hamamoto: Conceptualization (lead); Methodology (lead); writing – original draft (equal); formal analysis (lead); writing – review and editing (lead). M Gonda: Methodology (equal). K Taguchi: writing – review and editing (equal). Rei Unno: writing – review and editing (equal). Koei Torii: data curation (equal). M Isogai: data curation (equal). K Kawase: formal analysis (equal). T Nagai: writing – review and editing (equal). S Iwatsuki: Project administration. T Etani: Supervision. T Naiki: Supervision; writing – review and editing (equal). A Okada: Supervision. T Yasui: Supervision.

Funding statement

No funding.

Declarations

Competing interests

The authors declare no competing interests.

Additional information

Correspondence and requests for materials should be addressed to S.H.

Reprints and permissions information is available at www.nature.com/reprints.

Publisher's note Springer Nature remains neutral with regard to jurisdictional claims in published maps and institutional affiliations.

Open Access This article is licensed under a Creative Commons Attribution-NonCommercial-NoDerivatives 4.0 International License, which permits any non-commercial use, sharing, distribution and reproduction in any medium or format, as long as you give appropriate credit to the original author(s) and the source, provide a link to the Creative Commons licence, and indicate if you modified the licensed material. You do not have permission under this licence to share adapted material derived from this article or parts of it. The images or other third party material in this article are included in the article's Creative Commons licence, unless indicated otherwise in a credit line to the material. If material is not included in the article's Creative Commons licence and your intended use is not permitted by statutory regulation or exceeds the permitted use, you will need to obtain permission directly from the copyright holder. To view a copy of this licence, visit <http://creativecommons.org/licenses/by-nc-nd/4.0/>.

© The Author(s) 2024